Systems & Control Transactions

Original Research Article
Peer Reviewed Conference Proceeding
ESCAPE 36 - European Symposium on Computer Aided Process Engineering
Sheffield, UK. 21-24 June 2026

PSE PRESS

Global Optimization of Robust AC OPF

Yuhui Yin and Vassilis M. Charitopoulos*

Department of Chemical Engineering, Sargent Centre for Process Systems Engineering, UCL (University College London), Torrington Place, London WC1E 7JE, UK
* Corresponding Author: v.charitopoulos@ucl.ac.uk

ABSTRACT

Ensuring reliable operations of modern power systems under uncertainty remains a key challenge, particularly due to the non-convex nature of Alternating Current (AC) power flow equations and the presence of high-impact disturbances from load and renewable generation fluctuations. In this work, we address the robust AC Optimal Power Flow (AC OPF) problem by developing a robust spatial branch-and-bound (RsBB) algorithm. Robustness is achieved by identifying worst-case uncertainty realizations and iteratively incorporating robust cuts to eliminate constraint violations. To accelerate convergence and tighten bounds, Optimization-Based Bound Tightening (OBBT) and Feasibility-Based Bound Tightening (FBBT) techniques are integrated into the framework. The proposed method yields global robust solutions with certified optimality gaps below 0.01% across standard PGLib test cases.

Keywords: Nonconvex Robust Optimization, AC OPF, Cutting planes, Bound Tightening, Uncertainty, Global Optimization

INTRODUCTION

The AC optimal power flow (ACOPF) problem is a fundamental tool in power-system operations, computing minimum cost dispatch subject to power balance equations and network limits (e.g., voltage and thermal constraints) [1]. In practice, ACOPF is often solved deterministically using forecasts of demand and renewable injections. With the growing penetration of wind and solar, forecast errors can be substantial, so a deterministic operating point may violate constraints in real time (e.g., line overloads or voltage excursions) [2, 3]. Such violations jeopardize security and reliability and may push the system outside its secure operating limits. This motivates robust OPF formulations that remain feasible for all realizations of uncertainty within a prescribed set [4].

Existing OPF methods address uncertainty mainly via: (i) stochastic programming, which optimizes over sampled scenarios but can become computationally prohibitive as the number of scenarios grows, and is sensitive to scenario-generation and reduction errors [5, 6]; (ii) chance-constrained and distributionally robust chance-constrained models, which provide probabilistic security but typically rely on DC approximations or convex relaxations to gain tractability, thereby sacrificing exact AC feasibility and certifiable global optimality for the original nonconvex AC OPF [7, 8]; and (iii) robust optimization, which enforces feasibility for all uncertainty realizations, but in AC settings is still predominantly relaxation-based (SOCP/SDP/DC or convex restrictions), leading to conservatism and again losing guarantees of global optimality and exact AC feasibility [9-11].

Despite this progress, to the best of our knowledge there is still no method that simultaneously guarantees (a) robust feasibility for all values in a continuous uncertainty set and (b) certifiable global optimality for the full nonconvex ACOPF. Prior approaches either relax the AC physics or robustness to obtain tractability, or provide only scenario-based or probabilistic guarantees that do not cover the entire uncertainty set. This gap motivates the development of global-optimization framework tailored to robust ACOPF.

Such framework draws on several complementary lines of work. In semi-infinite global optimization, restriction and outer-approximation ideas provide a principled way to enforce constraints over continuous parameter domains [12]. In nonlinear robust optimization, generalized cutting-set procedures similarly generate many worst-case scenarios to certify feasibility over uncertainty sets [13]. On the algorithmic side, global solvers rely on systematic strengthening methods, including convex underestimators for trigonometric nonlinearities

[14] and optimality-based domain reduction to contract variable bounds during the search [15]. Complementing these methodological advances, recent power-system studies demonstrate that tailored global/MINLP strategies can be made effective at scale, e.g., for security-constrained unit commitment [16]. Together with broader developments in global optimization for MINLP [17], these ingredients provide the foundation for our robust spatial branch-and-cut approach for certifiable global robust ACOPF.

In this paper, we build on our previous work [18] and present a framework to globally solve the robust ACOPF via bound tightening and robust spatial branch-and-cut. The main contributions are as follows:

- BT–RsBB for global robust ACOPF: a robust spatial branch-and-cut scheme that iteratively refines convex relaxations while branching over the nonconvex region, converging to a globally robust optimal solution.
- Integrated bound tightening: a combination of optimization-based bound tightening (OBBT) and feasibility-based bound tightening (FBBT), where FBBT is applied within OBBT iterations to strengthen relaxations and shrink the search space at low overhead.
- Efficient trigonometric relaxations: an improved relaxation strategy that leverages precomputed sine-envelope parameters to rapidly generate tight linear relaxations of trigonometric constraints during the search.
- Parallel cut generation: concurrent generation of multiple cutting planes at nodes with uncertainty violations, improving node relaxations and accelerating pruning of robust-infeasible regions.

The remainder of the paper is organized as follows. Section **II** presents the ACOPF formulation and the relaxations used in the global algorithm. Section **III** details the robust spatial branch-and-cut procedure, including infeasibility testing, branching, cut generation, and bound tightening. Section **IV** reports numerical results and comparisons. Section **V** concludes.

PROBLEM FORMULATION

Deterministic AC-OPF (Polar Formulation)

We consider the standard AC optimal power flow (ACOPF) in polar coordinates, where each bus $k \in \mathcal{B}$ has voltage magnitude V_k and phase angle θ_k, and each generator $i \in \mathcal{G}$ controls real and reactive outputs (P_i^g, Q_i^g). Let (P_{km}, Q_{km}) denote the sending-end real/reactive line flows on branch $(k,m) \in \mathcal{L}$, with line parameters $(G_{km}, B_{km}, B_{km}^c)$[19]. The deterministic ACOPF minimizes a quadratic generation cost subject to (i) nodal real/reactive power balance (eq. 1b – 1c), (ii) voltage and generator operating limits (eq. 1d – 1f), (iii) nonlinear AC power-flow relations in polar form (eq. 1g), (iv) angle-difference bounds (eq. 1h), and (v) apparent-power (thermal) limits (eq. 1i). For compactness, we refer the interested read for the full formulation in [19-22], and succinctly present the problem below:

$$\min \sum_{i\in\mathcal{G}} \left(c_{2i}\left(P_i^g\right)^2 + c_{1i}P_i^g + c_{0i}\right) \tag{1a}$$

$$\text{s.t.} \sum_{i\in\mathcal{G}(k)} P_i^g - P_k^d - G_s V_k^2 = \sum_{km\in\mathcal{L}^{+(k)}} P_{km} + \sum_{km\in\mathcal{L}^{-(k)}} P_{mk}, \forall k \in \mathcal{B} \tag{1b}$$

$$\sum_{i\in\mathcal{G}(k)} Q_i^g - Q_k^d + B_s V_k^2 = \sum_{km\in\mathcal{L}^{+(k)}} Q_{km} + \sum_{km\in\mathcal{L}^{-(k)}} Q_{mk}, \forall k \in \mathcal{B} \tag{1c}$$

$$\underline{V}_k \le |V_k| \le \bar{V}_k, \forall k \in \mathcal{B} \tag{1d}$$

$$\underline{P}_i \le P_i^g \le \bar{P}_i, \forall i \in \mathcal{G} \tag{1e}$$

$$\underline{Q}_i \le Q_i^g \le \bar{Q}_i, \forall i \in \mathcal{G} \tag{1f}$$

$$c_{km} = V_k V_m cos(\theta_k - \theta_m), \forall (k,m) \in \mathcal{L} \tag{1g.1}$$

$$s_{km} = V_k V_m sin(\theta_k - \theta_m), \forall (k,m) \in \mathcal{L}$$

$$P_{km} = G_{km}V_k^2 - G_{km}c_{km} - B_{km}s_{km}, \forall (k,m) \in \mathcal{L} \tag{1g.2}$$

$$Q_{km} = -(B_{km} + B_{km}^c)V_k^2 - G_{km}s_{km} + B_{km}c_{km}, \forall (k,m) \in \mathcal{L} \tag{1g.3}$$

$$P_{mk} = G_{km}V_m^2 - G_{km}c_{km} + B_{km}s_{km}, \forall (k,m) \in \mathcal{L} \tag{1g.4}$$

$$Q_{mk} = -(B_{km} + B_{km}^c)V_m^2 + G_{km}s_{km} + B_{km}c_{km}, \forall (k,m) \in \mathcal{L} \tag{1g.5}$$

$$\theta_k - \theta_m \in \left[\underline{\theta}_{km}, \bar{\theta}_{km}\right], \forall (k,m) \in \mathcal{L} \tag{1h}$$

$$P_{km}^2 + Q_{km}^2 \le (\bar{S}_{km})^2, \forall (k,m) \in \mathcal{L} \tag{1i.1}$$

$$P_{mk}^2 + Q_{mk}^2 \le (\bar{S}_{km})^2, \forall (k,m) \in \mathcal{L} \tag{1i.2}$$

Note that, a reference angle constraint $\theta_{\text{ref}} = 0$ is imposed to ensure uniqueness of the polar representation [23].

Convex Relaxations for Global Optimization

We employ convex relaxations to provide valid lower

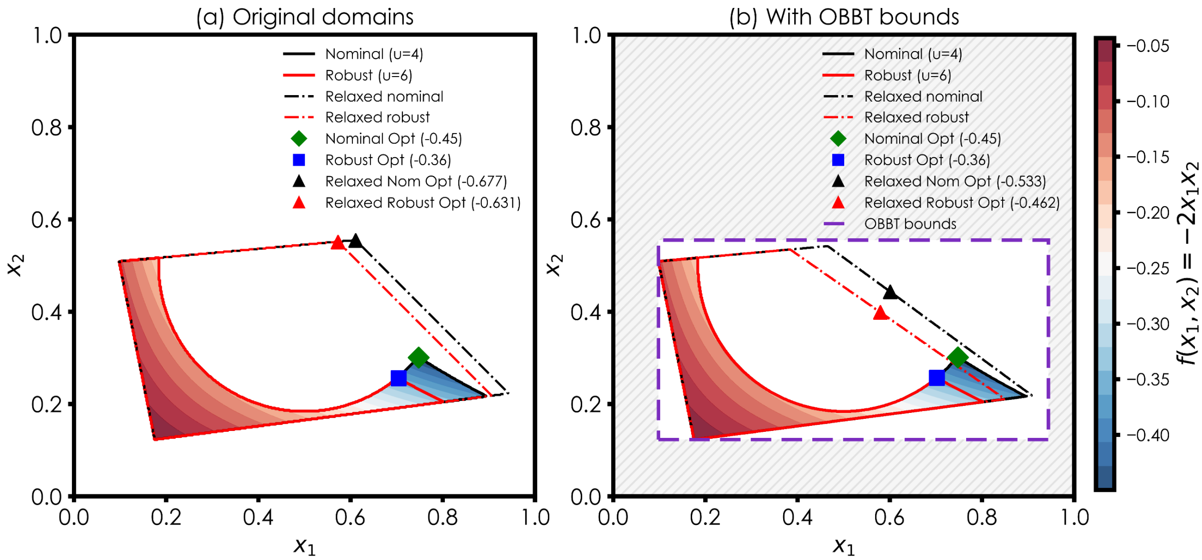

Figure 1. Illustration of the relationship between robust optimization and bound tightening: (a) original domains showing the nominal and robust feasible regions; (b) reduced domains after bound tightening, where the shaded region indicates the eliminated search space.

bounds within branch-and-bound. We adopt a quadratic-convex (QC) relaxation of the polar ACOPF [20, 22, 24]. The key idea is to lift the nonconvex bilinear and trigonometric terms and replace them with convex envelopes. In particular, we introduce lifted variables:

$$V_{km} \approx V_k V_m, V_{kk} \approx V_k^2, \cos_{km} \approx \cos(\theta_{km}) \tag{2}$$

$$\sin_{km} \approx \sin(\theta_{km}), \theta_{km} := \theta_k - \theta_m \tag{3}$$

We further define $\beta_{km}$and $\gamma_{km}$to represent the lifted products $V_{km}\cos_{km}$ and $V_{km}\sin_{km}$, respectively. Each lifted relation is relaxed using: (i) McCormick envelopes for bilinear products, (ii) convex quadratic envelopes for V_k^2, and (iii) convex/concave envelopes for $\sin(\cdot)$ and $\cos(\cdot)$ over the phase angle difference interval $\theta_{km} \in [\theta_{km}^l, \theta_{km}^u]$. Collectively, these constraints define a relaxation set $\mathcal{E}_{\mathrm{MC/QC}}(V^l, V^u, \theta^l, \theta^u)$. To further tighten the QC relaxation, we include a standard second-order cone (SOC) constraint

$$\beta_{km}^2 + \gamma_{km}^2 \leq V_{kk} V_{mm}, (k, m) \in \mathcal{L} \tag{4}$$

which couples the lifted terms and strengthens the QC bound.

Improved Trigonometric Relaxation

The tightness of the QC relaxation is often dominated by the quality of the envelopes related to the trigonometric functions present. Instead of a single generic sine envelope, we use a tighter piecewise outer approximation of $\sin(\theta)$ over $[\theta_{km}^l, \theta_{km}^u]$ that adapts to the interval sign pattern. Let the secant and tangent (supporting) lines be:

$$f^{\mathrm{sec}}(\theta^l, \theta^u) := \left(\frac{\sin(\theta^u) - \sin(\theta^l)}{\theta^u - \theta^l}\right)(\theta - \theta^l) + \sin(\theta^l) \tag{5}$$

$$f^{\tan}(t) := \sin(t) + \cos(t)(\theta - t) \tag{6}$$

If the interval does not cross zero, the global convexity/concavity of $\sin(\cdot)$yields a strong two-sided envelope. If $\theta_{km}^l < 0 < \theta_{km}^u$, we combine a secant with a small set of tangent supports (e.g., at an endpoint and a midpoint on each active side) to obtain a strictly tighter polyhedral outer approximation:

$$\begin{aligned} \sin_{km} &\leq f^{\mathrm{sec}}(\theta_{km}^l, \theta_{km}^u), \\ \sin_{km} &\geq \max\{ f^{\tan}(t) : t \in T_{km}\} \end{aligned} \tag{7}$$

(or the symmetric variant with reversed inequalities, depending on the interval regime). For efficiency within RsBB, the tangent locations T_{km} and any regime-dependent transition parameters are precomputed and stored; during branching and bounds tightening, only the active constraints for the detected region are enforced, while interval bounds are updated via mutable parameters. This construction yields tighter node relaxations and accelerates convergence by reducing feasible domains and strengthening lower bounds.

ROBUST OPTIMIZATION METHODOLOGY

We consider the original nonconvex robust optimization problem

Table 1: Quality and runtime results of robust ACOPF (optimality gaps are expressed in %). Results are obtained under a 1% perturbation. Times are CPU seconds. For BT–RsBB, the reported time is shown as the summation of bound-tightening time and subsequent RsBB time. IR denotes the improved relaxation and RR denotes the reference relaxation.

Box uncertainty								
	Optimality gap (%)				CPU (s)			
Case	RsBB		BT-RsBB		RsBB		BT-RsBB	
	IR	RR	IR	RR	IR	RR	IR	RR
case3_lmbd	0.010	0.010	0.009	0.009	54.0	55.1	19.0	13.4
Case5_pjm	10.633	10.765	0.030	0.034	7200.0	7200.1	7200.0	7200.0
case14 ieee	0.034	0.034	0.009	0.009	7200.0	7200.0	27.2	26.2
case30 as	0.049	0.049	0.008	0.008	7200.0	7201.0	3160.5	3305.2
case73 ieee rts	0.026	0.026	0.010	0.010	7200.4	7200.0	258.2	246.7
case197 snem	0.030	0.030	0.010	0.010	7200.0	7202.0	1952.6	7200.0

Polyhedral uncertainty								
	Optimality gap (%)				CPU (s)			
Case	RsBB		BT-RsBB		RsBB		BT-RsBB	
	IR	RR	IR	RR	IR	RR	IR	RR
case3_lmbd	0.010	0.010	0.007	0.007	55.3	53.5	16.6	17.8
Case5_pjm	10.778	10.846	0.030	0.035	7200.0	7200.1	7200.0	7200.0
case14 ieee	0.034	0.034	0.009	0.009	7200.0	7200.0	33.0	29.8
case30 as	0.049	0.049	0.008	0.008	7200.0	7201.0	3127.1	3330.7
case73 ieee rts	0.027	0.027	0.010	0.010	7200.0	7209.9	258.1	245.6
case197 snem	0.030	0.030	0.010	0.010	7200.0	7201.1	1887.2	7200.4

$$\min_{x\in\mathcal{X}} f(x) \ \text{s.t.}\ g(x,u)\le 0, \forall u\in\mathcal{U}, \tag{8}$$

where x denotes the decision variables, $\mathcal{X}$ is a bounded feasible region, u is an uncertain parameter lying in a prescribed uncertainty set $\mathcal{U}$, and $g(\cdot,\cdot)$ collects the uncertain constraints. Since global solution of (8) is challenging for nonconvex models, we adopt the robust spatial branch-and-bound (RsBB) framework in [25], which provides finite convergence to a globally robust optimal solution under standard regularity assumptions (boundedness, continuity, and tractability of the inner maximization).

RsBB Framework: Master Problems and Infeasibility Test

At each spatial branch-and-bound node, RsBB maintains: (i) a nonconvex master problem that enforces robustness over a current finite subset of uncertainty realizations, and (ii) a convex relaxation that yields valid lower bounds. Specifically, for a cutting-set $\hat{\mathcal{U}}\subseteq\mathcal{U}$, the node master is

$$(P_{\text{nonc}})\min_{x\in\mathcal{X}} f(x) \ \text{s.t.}\ g(x,u)\le 0, \forall u\in\hat{\mathcal{U}}, \tag{9}$$

whose robust-feasible solutions provide incumbents (upper bounds). Next, we solve a convex relaxation

$$(P_{\text{conv}})\min_{x\in\mathcal{X}} f_{\text{conv}}(x) \ \text{s.t.}\ g_{\text{conv}}(x,u)\le 0, \forall u\in\hat{\mathcal{U}}, \tag{10}$$

where f_{conv} and g_{conv} are convex relaxations of f and g. The optimal value of P_{conv} is a valid node lower bound, and the global lower bound is the minimum across open nodes, as in standard spatial B&B [25].

Robust feasibility of a candidate x^* from P_{nonc} is checked by an infeasibility test (inner maximization)

$$(P_{\text{it}})\ \max_{u\in\mathcal{U}} g(x^*,u), \tag{11}$$

which returns a worst-case realization u^*. If $g(x^*,u^*)>\varepsilon_{\text{it}}$, then x^* is not robustly feasible and the violating scenario u^* is added to $\hat{\mathcal{U}}$ (equivalently, we append the cut $g(x,u^*)\le 0$ to both P_{nonc} and P_{conv} at the node). This cutting-set loop is repeated until no violation is found (within ε_{it}), after which the resulting x^* is robust-feasible over $\mathcal{U}$ up to tolerance. The outer spatial branching loop guarantees global optimality by maintaining valid bounds and partitioning variable domains; full algorithmic details and convergence arguments follow [25].

Uncertainty in AC OPF

In this work, uncertainty enters through bus

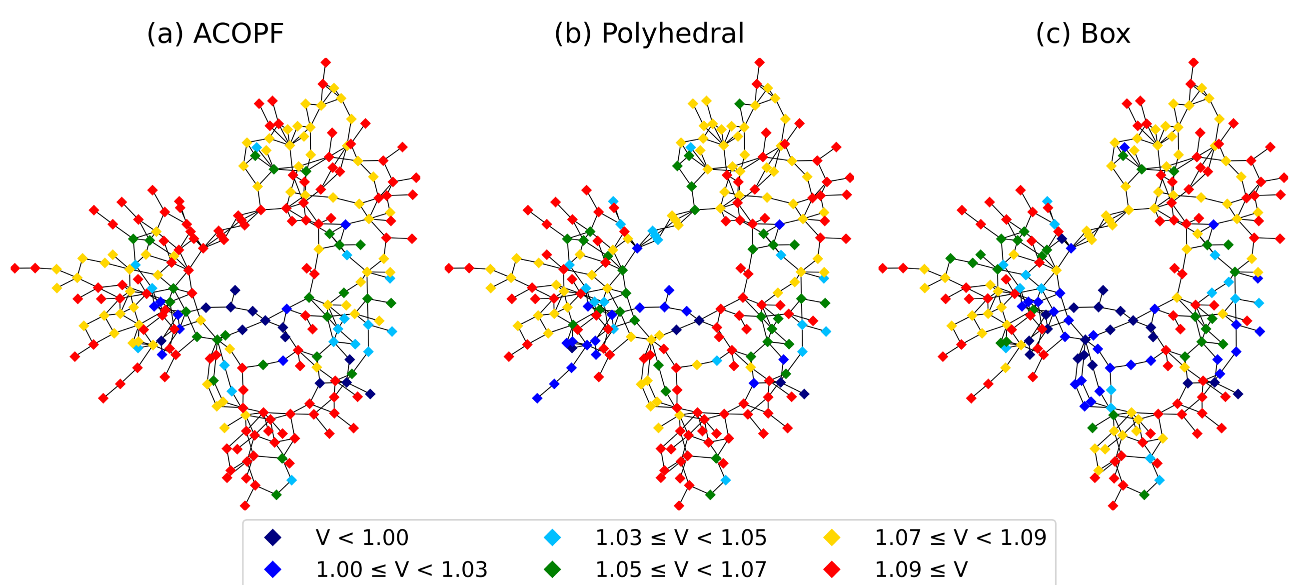

Figure 2. Voltage magnitude profiles for case240_pserc: (a) nominal ACOPF solution without uncertainty, (b) robust ACOPF under polyhedral uncertainty, and (c) robust ACOPF under box uncertainty, obtained by BT–RsBB with the improved relaxation. Bus colors indicate voltage bins (p.u).

demands. Let $(P^d_{k,\text{nom}}, Q^d_{k,\text{nom}})$ be nominal loads and define

$$\tilde{P}^d_k = (1+\xi_k)P^d_{k,\text{nom}},\ \tilde{Q}^d_k = (1+\xi_k)Q^d_{k,\text{nom}}, \xi \in \mathcal{U}. \tag{9}$$

We consider standard convex uncertainty sets, either a box $\mathcal{U}_{\text{box}} = \{\xi : |\xi_k| \le \Psi_k, \forall k\}$, or a budgeted polyhedral set $\mathcal{U}_{\text{poly}} = \{\xi : |\xi_k| \le \Psi_k, \forall k, \sum_{k\in\mathcal{B}} |\xi_k| \le \Gamma\}$. Robustness is enforced by replacing the (deterministic) active/reactive power-balance equalities in (1) with robust constraints $\forall \xi \in \mathcal{U}$, and update violated constraints via P_{it} as described above. In our implementation, the inner maximization is solved using the current candidate operating point $(P^{g*}, Q^{g*}, V^*, \theta^*, \ldots)$, and any violating realization ξ^* generates a cut corresponding to the power-balance constraint at ξ^*.

Bounds Tightening

To accelerate RsBB on the nonconvex AC OPF, we apply bound tightening to strengthen relaxations without materially increasing model size. As shown in Figure. 1, tightening contracts the variable domains and removes portions of the search space that cannot contain feasible solutions, thereby improve relaxation strength and reduce the need for branching. We use:

- **Feasibility-based bound tightening (FBBT):** inexpensive constraint propagation applied to the relaxation to remove infeasible portions of variable domains.
- **Optimization-based bound tightening (OBBT):** stronger tightening obtained by solving auxiliary minimization/maximization subproblems over the current convex relaxation to contract selected variable bounds (here, primarily V_k and θ_{km}).

FBBT is applied as preprocessing and after OBBT to propagate improvements through the constraint set. The resulting tighter bounds improve the quality of QC relaxations, reduce branching, and speed up convergence of the robust global algorithm.

NUMERICAL RESULTS

We evaluate the proposed robust ACOPF framework on benchmark networks and study three factors: (i) the effect of uncertainty set choice (nominal vs. box vs. polyhedral), (ii) the impact of bound tightening (RsBB vs. BT–RsBB), and (iii) the benefit of the improved trigonometric relaxation relative to a reference sine relaxation.

Test Cases and Computational Setting

Experiments are conducted on 17 test cases from PGLib-OPF [26] with fewer than 500 buses. Active and reactive demands are perturbed by $\xi_k \in [-0.01, 0.01]$ (1% level). We consider box $\mathcal{U}_{box} = \{\xi : |\xi_k| \le \Psi_k, \forall k\}$ and polyhedral set $\mathcal{U}_{\text{poly}} = \{\xi : |\xi_k| \le \Psi_k, \forall k, \sum_{k\in\mathcal{B}} |\xi_k| \le \Gamma\}$, and also report the deterministic nominal case. All models are implemented in Pyomo 6.9.2 (Python 3.10.18). Nonconvex NLP sub-problems are solved with IPOPT (tolerance 10^{-8}). The infeasibility test uses $\varepsilon_{\text{it}} = 10^{-4}$, and RsBB termination/fathoming uses a global relative tolerance $\varepsilon = 10^{-4}$. Bound tightening uses a hybrid FBBT + OBBT procedure with $\varepsilon_{\text{bt}} = 10^{-2}$ and at most 10 iterations; OBBT subproblems are run in parallel on 16 cores. Each RsBB

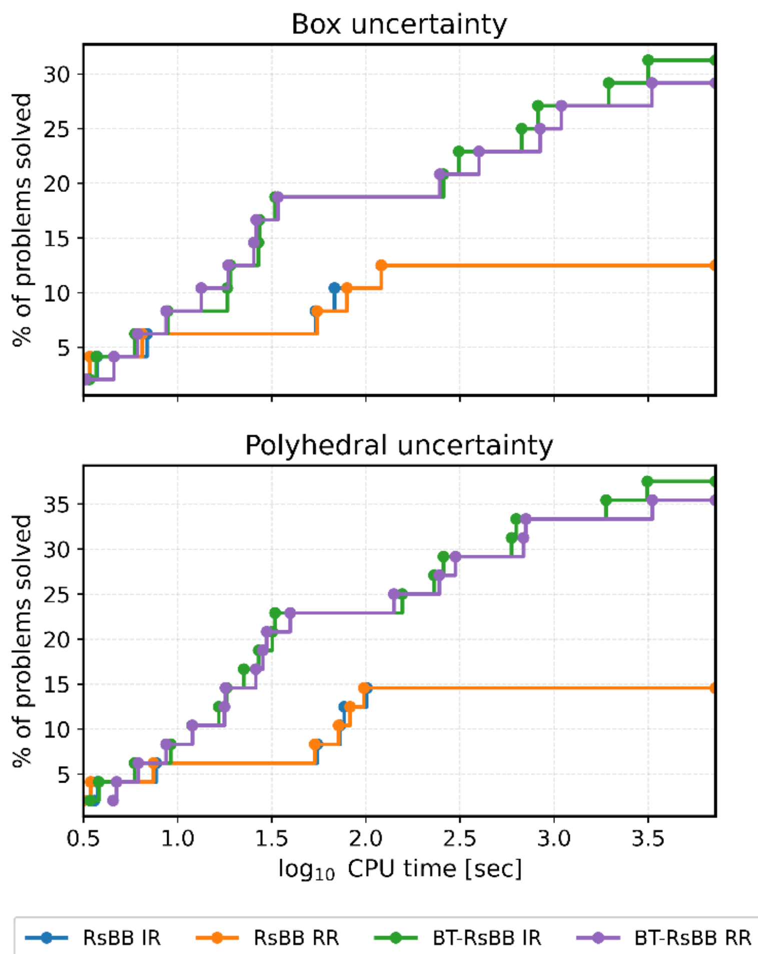

Figure 3. Percentage of instances certified within a given CPU time (log-scale) under a 2h time limit (7200 s). Curves compare RsBB vs. BT–RsBB with the improved relaxation (IR) and the reference relaxation (RR).

run has a 2 h time limit. Experiments are executed on a Windows workstation (Intel Core Ultra 7, 32GB).

Robust Operating Points and Computational Tractability

Table 1 reports robust AC OPF benchmark results under a 1% demand perturbation ($\xi = 0.01$) for both box and polyhedral uncertainty sets. For each test case, we compare RsBB against BT–RsBB (with FBBT+OBBT), and we also compare the improved relaxation (IR) with the reference relaxation (RR). Reported gaps are relative robust optimality gaps (in %), and times are CPU seconds (stopped at the 2h limit).

Overall, BT–RsBB consistently yields smaller gaps and/or more solved instances within the time limit than pure RsBB, confirming that bound tightening strengthens the relaxations and reduces the required branching effort. Across both uncertainty sets, IR tends to achieve smaller final gaps than RR for comparable runtimes, or reaches similar gaps faster, indicating that tighter trigonometric envelopes improve lower bounds and accelerate convergence. Finally, polyhedral uncertainty is generally easier than box uncertainty, since the budgeted structure is less conservative and typically produces weaker worst-case violations, leading to a smaller and faster global search.

Figure 2 illustrates the voltage magnitude profile for case240_pserc under: (a) nominal ACOPF, (b) polyhedral robustness, and (c) box robustness (BT–RsBB with the improved relaxation). Compared with the nominal dispatch, robust solutions reshape the voltage profile to preserve feasibility under demand deviations. The box robust solution is visibly more conservative than the polyhedral one, consistent with the fact that $\mathcal{U}_{\text{box}}$ allows simultaneous worst-case deviations at all buses, while $\mathcal{U}_{\text{poly}}$ limits the deviation via a budget Γ.

Figure 3 reports empirical solve-rate curves (fraction of instances certified globally optimal within a given CPU time, log-scale) for RsBB and BT–RsBB under both uncertainty sets, using either the improved relaxation (IR) or the reference relaxation (RR).

Three trends are consistent across the benchmark suite:

- **Bound tightening is the main accelerator.** BT–RsBB solves substantially more instances than baseline RsBB within the 2 h limit. Tightened bounds shrink the search space and strengthen node relaxations, leading to fewer branch-and-bound nodes and faster gap closure.
- I**mproved trigonometric relaxation provides additional speedups.** IR yields systematically faster convergence than RR, reflecting tighter lower bounds and reduced relaxation error in the lifted sine/cosine constraints. The effect is moderate on the log-time plot but corresponds to noticeable reductions in wall-clock time on solved cases.
- **Polyhedral uncertainty is less conservative and easier computationally than box uncertainty.** Under Upoly, more instances are certified within the time limit. The budget constraint limits extremal scenarios, typically requiring fewer robust cuts and producing smaller search trees than the harsher Ubox setting. Overall, the numerical results indicate that combining RsBB with hybrid bound tightening is critical for scalability on robust ACOPF, while tighter trigonometric envelopes further improve performance. The choice of uncertainty set strongly affects both conservatism and computational difficulty, with box uncertainty being the most demanding.

CONCLUSION

In this paper, we developed an enhanced BT–RsBB framework to compute globally robust optimal solutions for nonconvex ACOPF under uncertainty. Building on the RsBB methodology, we improve practical efficiency via (i) parallel robust-cut generation in the infeasibility test, (ii) a hybrid bound-tightening module combining FBBT and OBBT, and (iii) a tighter trigonometric relaxation based on a precomputed mapping that strengthens node relaxations without substantially increasing model size.

We evaluate the method on 48 PGLib-OPF benchmark networks under three operating conditions (TYP, API, SAD) with both box and budgeted polyhedral uncertainty sets. The results show that BT–RsBB consistently outperforms baseline RsBB: bound tightening significantly contracts variable domains, strengthens relaxations, and accelerates robust gap closure, yielding more certified solutions within a two-hour limit. The improved sine relaxation further reduces runtimes by tightening lower bounds and decreasing the number of explored nodes.

The study also reveals strong sensitivity to operating conditions and uncertainty set geometry. Box uncertainty is systematically more conservative—and typically harder—than polyhedral uncertainty because it permits simultaneous worst-case deviations at all buses. Overall, our results provide a rigorous global benchmark for robust ACOPF with certified bounds and transparent convergence behaviour. Future work will target scalability through adaptive bound tightening, stronger branching and range-reduction strategies, and learning-based acceleration for cut selection, node selection, and relaxation refinement.

DATA AVAILABILITY

The data underlying this article will be shared on reasonable request to the corresponding author.

ACKNOWLEDGEMENTS

Financial support from EPSRC grants EP/T022930/1, EP/W003317/1 and EP/V051008/1 and UCL's Research Excellence Scholarship is gratefully acknowledged.

AUTHOR IDENTIFIERS

Author ORCIDs:
Charitopoulos VM: 0000-0001-9051-917X
Yuhui Y: 0009-0000-5360-720X

REFERENCES

1. Carpentier J. Contribution à l'étude du dispatching économique. Bulletin de la Société Française des Électriciens 3(1):431–447 (1962).
2. Phan D, Ghosh S. Two-stage stochastic optimization for optimal power flow under renewable generation uncertainty. ACM Trans. Model. Comput. Simul. 24:1-22 (2014). https://doi.org/10.1145/2553084
3. Louca R, Bitar E. Robust AC optimal power flow. IEEE Trans. Power Syst. 34:1669-1681 (2019). https://doi.org/10.1109/tpwrs.2018.2849581
4. Lee D, Turitsyn K, Molzahn DK, Roald LA. Robust AC optimal power flow with robust convex restriction. IEEE Trans. Power Syst. 36:4953-4966 (2021). https://doi.org/10.1109/tpwrs.2021.3075925
5. Papavasiliou A, Oren SS, O'Neill RP. Reserve requirements for wind power integration: a scenario-based stochastic programming framework. IEEE Trans. Power Syst. 26:2197-2206 (2011). https://doi.org/10.1109/tpwrs.2011.2121095
6. Marley JF, Vrakopoulou M, Hiskens IA. An AC-QP optimal power flow algorithm considering wind

forecast uncertainty. 2016 IEEE Innovative Smart Grid Technologies - Asia (ISGT-Asia) :317-323 (2016). https://doi.org/10.1109/isgt-asia.2016.7796405
7. Venzke A, Halilbasic L, Markovic U, Hug G, Chatzivasileiadis S. Convex relaxations of chance constrained AC optimal power flow. IEEE Trans. Power Syst. 33:2829-2841 (2018). https://doi.org/10.1109/tpwrs.2017.2760699
8. Arab A, Tate JE. Distributionally robust optimal power flow via ellipsoidal approximation. IEEE Trans. Power Syst. 38:4826-4839 (2023). https://doi.org/10.1109/tpwrs.2022.3217941
9. Bai X, Qu L, Qiao W. Robust AC optimal power flow for power networks with wind power generation. IEEE Trans. Power Syst. 31:4163-4164 (2016). https://doi.org/10.1109/tpwrs.2015.2493778
10. Louca R, Bitar E. Robust AC optimal power flow. IEEE Trans. Power Syst. 34:1669-1681 (2019). https://doi.org/10.1109/tpwrs.2018.2849581
11. Yang H, Morton DP, Bandi C, Dvijotham K. Robust optimization for electricity generation. INFORMS Journal on Computing 33:336-351 (2021). https://doi.org/10.1287/ijoc.2020.0956
12. Mitsos A. Global optimization of semi-infinite programs via restriction of the right-hand side. Optimization 60:1291-1308 (2011). https://doi.org/10.1080/02331934.2010.527970
13. Isenberg NM, Akula P, Eslick JC, Bhattacharyya D, Miller DC, Gounaris CE. A generalized cutting?set approach for nonlinear robust optimization in process systems engineering. AIChE Journal 67: (2021). https://doi.org/10.1002/aic.17175
14. Caratzoulas S, Floudas CA. Trigonometric convex underestimator for the base functions in fourier space. J Optim Theory Appl 124:339-362 (2005). https://doi.org/10.1007/s10957-004-0940-2
15. Zhang Y, Sahinidis NV, Nohra C, Rong G. Optimality-based domain reduction for inequality-constrained NLP and MINLP problems. J Glob Optim 77:425-454 (2020). https://doi.org/10.1007/s10898-020-00886-z
16. Castelli, A. F., Harjunkoski, I., Poland, J., Giuntoli, M., Martelli, E., & Grossmann, I. E. (2024). Solving the security constrained unit commitment problem: Three novel approaches. *Int. J. Electr. Pow. Energy Sys.*, *162*, 110213.
17. Boukouvala F, Misener R, Floudas CA. Global optimization advances in mixed-integer nonlinear programming, MINLP, and constrained derivative-free optimization, CDFO. European Journal of Operational Research 252:701-727 (2016). https://doi.org/10.1016/j.ejor.2015.12.018
18. Marousi A, Charitopoulos VM. Global robust optimisation for non-convex quadratic programs: application to pooling problems. Systems and Control Transactions 4:1592-1597 (2025). https://doi.org/10.69997/sct.168949
19. Zimmerman RD, Murillo-Sánchez CE. MATPOWER user's manual. *Power Systems Engineering Research Center* (2016). [Online].
20. Available: https://matpower.org/docs/MATPOWER-manual.pdf https://doi.org/10.5281/zenodo.3236519
21. Coffrin C, Hijazi HL, Van Hentenryck P. Strengthening the SDP relaxation of AC power flows with convex envelopes, bound tightening, and valid inequalities. IEEE Trans. Power Syst. 32:3549-3558 (2017). https://doi.org/10.1109/tpwrs.2016.2634586
22. Taylor JA. Convex optimization of power systems. *Cambridge University Press* (2015).
23. Coffrin C, Hijazi HL, Van Hentenryck P. The QC relaxation: a theoretical and computational study on optimal power flow. IEEE Trans. Power Syst. 31:3008-3018 (2016). https://doi.org/10.1109/tpwrs.2015.2463111
24. Bynum M, Castillo A, Watson JP, Laird CD. Tightening mccormick relaxations toward global solution of the ACOPF problem. IEEE Trans. Power Syst. 34:814-817 (2019). https://doi.org/10.1109/tpwrs.2018.2877099
25. Chen C, Atamturk A, Oren SS. Bound tightening for the alternating current optimal power flow problem. IEEE Trans. Power Syst. 31:3729-3736 (2016). https://doi.org/10.1109/tpwrs.2015.2497160
26. Marousi A, Charitopoulos VM. Global and robust optimisation for non-convex quadratic programs. arXiv preprint (2025). https://arxiv.org/abs/2503.07310
27. Babaeinejadsarookolaee S, Birchfield A, Christie RD, Coffrin C, DeMarco C, Diao R, Ferris M, Fliscounakis S, Greene S, Huang R, et al. The power grid library for benchmarking AC optimal power flow algorithms. arXiv preprint(2019). https://arxiv.org/abs/1908.02788